Vol 18 No 8, August 2009
1674-1056/2009/18(08)/3597-08

Chinese Physics B

© 2009 Chin. Phys. Soc.
and IOP Publishing Ltd

Accurate and rapid error estimation on global gravitational field from current GRACE and future GRACE Follow-On missions*

Zheng Wei(郑 伟)[a)b)†], Hsu Hou-Tse(许厚泽)[a)], Zhong Min(钟 敏)[a)], and Yun Mei-Juan(员美娟)[c)]

[a)] *Key Laboratory of Dynamic Geodesy, Institute of Geodesy and Geophysics, Chinese Academy of Sciences, Wuhan 430077, China*

[b)] *Disaster Prevention Research Institute, Kyoto University, Uji, Kyoto 611-0011, Japan*

[c)] *Department of Applied Physics, Wuhan University of Science and Technology, Wuhan 430081, China*

(Received 17 November 2008; revised manuscript received 20 December 2008)

Firstly, the new combined error model of cumulative geoid height influenced by four error sources, including the inter-satellite range-rate of an interferometric laser (K-band) ranging system, the orbital position and velocity of a global positioning system (GPS) receiver and non-conservative force of an accelerometer, is established from the perspectives of the power spectrum principle in physics using the semi-analytical approach. Secondly, the accuracy of the global gravitational field is accurately and rapidly estimated based on the combined error model; the cumulative geoid height error is 1.985×10^{-1} m at degree 120 based on GRACE Level 1B measured observation errors of the year 2007 published by the US Jet Propulsion Laboratory (JPL), and the cumulative geoid height error is 5.825×10^{-2} m at degree 360 using GRACE Follow-On orbital altitude 250 km and inter-satellite range 50 km. The matching relationship of accuracy indexes from GRACE Follow-On key payloads is brought forward, and the dependability of the combined error model is validated. Finally, the feasibility of high-accuracy and high-resolution global gravitational field estimation from GRACE Follow-On is demonstrated based on different satellite orbital altitudes.

Keywords: global gravitational field, GRACE Follow-On, semi-analytical approach, combined error model

PACC: 9110, 9480R, 0420M

1. Introduction

Since the Italian physicist Galileo determined gravity for the first time at the end of the 16th century, an army of international researchers have accomplished all sorts of gravity studies.[1−24] The Earth's static and time-varying gravitational field is a physical field which can reflect the spatial distribution, movement and change of materials on and inside of the Earth, and can dominate the undulation and change of geoid.[25] Accordingly, the investigation of the detailed configuration and time-variable characteristics of the Earth's gravitational field is not only to satisfy the requirements for geophysics, geodesy, oceanography, seismology, space science, national defense and so on, but will also provide important information for resource exploration, environmental protection and disaster monitoring.[26,27] The Gravity Recovery And Climate Experiment (GRACE) satellites launched successfully and GRACE Follow-On to be launched (shown in Table 1) declare that human beings will meet the era of unprecedented satellite gravity exploration.

The GRACE satellites researched cooperatively by the American National Aeronautics and Space Administration (NASA) and the German Das Deutsche Zentrum für Luft- und Raumfahrt (DLR) are designed to have an almost circular and near polar orbit, and high-accuracy measurement of inter-satellite range-rate by the K-band ranging system, of orbital position and velocity by high-orbiting global positioning system (GPS) satellites and of non-conservative forces (atmospheric drag, solar radiation pressure, Earth's albedo, orbital

*Project supported by the National Natural Science Foundation of China (Grant No 40674038), the Funds of the Chinese Academy of Sciences for Key Topics in Innovation Engineering (Grant Nos KZCX2-YW-143 and KZCX2-YW-202), the National High Technology Research and Development Program of China (863) (Grant Nos 2009AA12Z138 and 2006AA09Z153) and the Grant-in-Aid for Scientific Research of Japan (Grant No B19340129).

†Corresponding author. E-mail: wzheng@asch.whigg.ac.cn

altitude and attitude control forces and so on) by the SuperSTAR accelerometer. GRACE not only includes two groups of the satellite-to-satellite tracking in the high–low mode (SST-HL), but also determines the mutual movements of two low-orbiting satellites based on the differential principle. Accordingly, the accuracy of the static and time-variable GRACE global gravitational field is at least one order of magnitude higher than that of the CHAllenging Minisatellite Payload (CHAMP) satellite, and GRACE will establish a stable foundation for high-accuracy measurement from the gravity field and steady-state ocean circulation explorer (GOCE) satellite.

Table 1. A comparison between GRACE and GRACE Follow-On missions.

parameters	indexes	
	GRACE	GRACE Follow-On
country	America and Germany	America
organization	NASA and DLR	NASA
launch time	2002.3.17	2013
lifetime	5–10 y	>2 y
orbital altitude	500–300 km	~ 250 km
orbital inclination	89°	89°
orbital eccentricity	<0.004	<0.004
inter-satellite range	220 km	50 km
spatial resolution	166 km	55 km

Based on the excellent behaviors of the high-accuracy measurement of the medium–long wave global gravitational field from GRACE, NASA brought forward another dedicated future satellite mission named GRACE Follow-On to determine with high-accuratcy the medium–short wave global gravitational field.[28,29] GRACE Follow-On, designed as an almost circular, near polar and low Earth orbit, measures with high-accuracy the inter-satellite range-rate by an interferometric laser ranging system, the orbital position and velocity by high-orbiting GPS satellites and the non-conservative force by an accelerometer, and compensates the non-conservative force by a drag-free control system. Accordingly, the accuracy of static and time-variable GRACE Follow-On global gravitational field is at least one order of magnitude higher than that of GRACE.

The semi-analytical approach is one of the effective methods to estimate the accuracies of GRACE and GRACE Follow-On global gravitational field. The advantages are that the physical meaning of the satellite observation equation is definite, the error is analyzed easily, and the high-degree global gravitational field can be solved rapidly. Recently, an army of researchers has acquired illustrious fruits on estimating to high-accuracy the global gravitational field using the semi-analytical approach. Jekeli and Rapp[30] built the single error model of cumulative geoid height, influenced only by inter-satellite range-rate error; however, the influences of orbital position, orbital velocity and non-conservative force errors were not considered in their studies. Thereby, the accuracy of the global gravitational field can only be estimated approximately. Differently from previous studies, we establish, for the first time so far as we know, the combined error model of cumulative geoid height influenced by four error sources including inter-satellite range-rate, orbital position, orbital velocity and non-conservative force from the view of the power spectrum principle in physics using the semi-analytical approach; the matching relationship of accuracy indexes from GRACE Follow-On key payloads is brought forward; the feasibility of high-accuracy global gravitational field estimation from GRACE Follow-On is demonstrated using different orbital altitudes. Therefore, the accuracies of GRACE and GRACE Follow-On global gravitational field can be accurately estimated based on the combined error model in this paper.

2. Methods

2.1. Inter-satellite range-rate error model

The disturbing geopotential $T(r,\phi,\lambda)$ can be defined as

$$T(r,\phi,\lambda)=\frac{GM}{r}\sum_{l=2}^{L}\sum_{m=0}^{l}\left[\left(\frac{R_{\rm e}}{r}\right)^{l}(\bar{C}_{lm}\cos m\lambda + \bar{S}_{lm}\sin m\lambda)\bar{\rm P}_{lm}(\sin\phi)\right], \quad (1)$$

where r is the distance from satellite centroid to the geocentre, ϕ and λ are respectively geocentric latitude and longitude, GM is the product of the Earth's mass M and gravitational constant G, $R_{\rm e}$ represents the Earth's mean radius, $\bar{\rm P}_{lm}(\sin\phi)$ denotes the normalized Legendre polynomial with degree l and order m, and $\bar{C}_{lm}$ and $\bar{S}_{lm}$ are the estimated and normalized geopotential coefficients.

The power spectrum of $T(r,\phi,\lambda)$ is expressed as

$$P_l^2\{T(r,\phi,\lambda)\} = \sum_{m=0}^{l}\left[\frac{1}{4\pi}\iint T(r,\phi,\lambda)\bar{\rm Y}_{lm}(\phi,\lambda)\cos\phi{\rm d}\phi{\rm d}\lambda\right]^2, \tag{2}$$

where $\bar{\rm Y}_{lm}(\phi,\lambda) = \bar{\rm P}_{l|m|}(\sin\phi)Q_m(\lambda)$, $Q_m(\lambda) = \begin{cases}\cos m\lambda & m\geq 0,\\ \sin|m|\,\lambda & m<0.\end{cases}$

Based on orthogonality of the spherical harmonic function, equation (2) is simplified as

$$P_l^2\{T(r,\phi,\lambda)\} = \left(\frac{GM}{R_{\rm e}}\right)^2\left(\frac{R_{\rm e}}{r}\right)^{2l+2} \times\sum_{m=0}^{l}(\bar{C}_{lm}^2+\bar{S}_{lm}^2). \tag{3}$$

The power spectrum of the geoid can be represented as

$$P_l^2\{N\} = R_{\rm e}^2\sum_{m=0}^{l}(\bar{C}_{lm}^2+\bar{S}_{lm}^2). \tag{4}$$

Combining Eq.(3) with Eq.(4), the relationship between $P_l^2\{N\}$ and $P_l^2\{T(r,\phi,\lambda)\}$ is obtained as

$$P_l^2\{N\} = R_{\rm e}^2\left(\frac{R_{\rm e}}{GM}\right)^2\left(\frac{r}{R_{\rm e}}\right)^{2l+2}P_l^2\{T(r,\phi,\lambda)\}. \tag{5}$$

In the spherical coordinate system, the partial derivatives of $T(r,\phi,\lambda)$ with respect to ϕ and λ can be shown as

$$\begin{aligned}\frac{\partial T(r,\phi,\lambda)}{\partial\phi} &= \frac{GM}{r}\sum_{l=2}^{L}\sum_{m=0}^{l}\left[\left(\frac{R_{\rm e}}{r}\right)^l(\bar{C}_{lm}\cos m\lambda+\bar{S}_{lm}\sin m\lambda)(\bar{\rm P}_{l,m+1}(\sin\phi)-m\,{\rm tg}\,\phi\bar{\rm P}_{lm}(\sin\phi))\right],\\ \frac{\partial T(r,\phi,\lambda)}{\partial\lambda} &= \frac{GM}{r}\sum_{l=2}^{L}\sum_{m=0}^{l}\left[\left(\frac{R_{\rm e}}{r}\right)^l(-m\bar{C}_{lm}\sin m\lambda+m\bar{S}_{lm}\cos m\lambda)\bar{\rm P}_{lm}(\sin\phi)\right].\end{aligned} \tag{6}$$

As shown in Fig.1, the asterisk, solid and circled lines are $P_l^2\{T(r,\phi,\lambda)\}$, $P_l^2\{\partial T(r,\phi,\lambda)/\partial\phi\}$ and $P_l^2\{\partial T(r,\phi,\lambda)/\partial\lambda\}$, respectively. The relationship between $P_l^2\{\partial T(r,\phi,\lambda)/\partial\lambda\}$ is given by

$$\begin{aligned}P_l^2\{\partial T(r,\phi,\lambda)/\partial\lambda\} &= \left(\frac{GM}{R_{\rm e}}\right)^2\left(\frac{R_{\rm e}}{r}\right)^{2l+2}\\ &\quad\times\sum_{m=0}^{l}m^2(\bar{C}_{lm}^2+\bar{S}_{lm}^2)\\ &= \frac{l^2}{2}P_l^2\{T(r,\phi,\lambda)\}.\end{aligned} \tag{7}$$

Due to spherical symmetry, $P_l^2\{\partial T(r,\phi,\lambda)/\partial\phi\}$ is the same with $P_l^2\{\partial T(r,\phi,\lambda)/\partial\lambda\}$

$$\begin{aligned}P_l^2\left\{\frac{\partial T(r,\phi,\lambda)}{\partial\phi}\right\} &= P_l^2\left\{\frac{\partial T(r,\phi,\lambda)}{\partial\lambda}\right\}\\ &= \frac{l^2}{2}P_l^2\{T(r,\phi,\lambda)\}.\end{aligned} \tag{8}$$

Based on the energy conservation principle in physics, the observation equation of single satellite can be defined as

$$\frac{1}{2}\dot{\boldsymbol{r}}^2 = V_0+T+C, \tag{9}$$

where $\dot{\boldsymbol{r}}$ is the velocity vector, V_0 denotes the geocentric potential, and C is the energy constant.

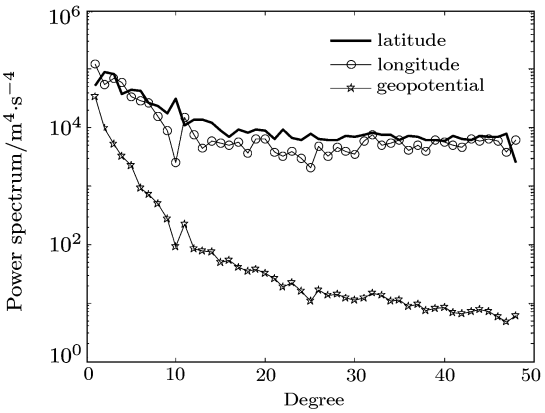


Fig.1. Power spectrum of $T(r,\phi,\lambda)$, $\partial T(r,\phi,\lambda)/\partial\phi$ and $\partial T(r,\phi,\lambda)/\partial\lambda$ at each degree.

As shown in Fig.2, O–XYZ denotes the Earth-centered inertial (ECI) frame, the observation equa-

tion of twin satellites is expressed as

$$\frac{1}{2}(\dot{r}_2+\dot{r}_1)\dot{\rho}_{12}=T_2-T_1, \tag{10}$$

where $\frac{1}{2}(\dot{r}_2+\dot{r}_1)=\sqrt{GM/r}$ denotes the mean velocity

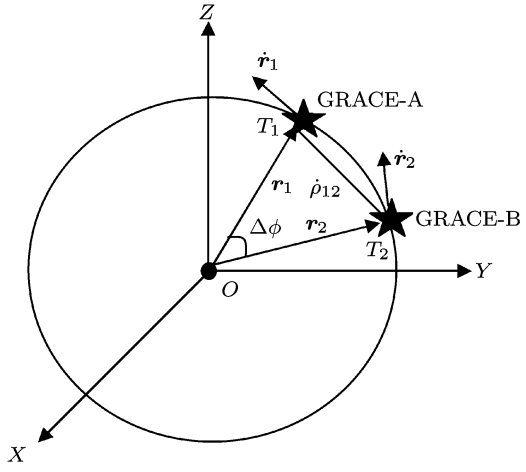


Fig.2. In-orbit flight of GRACE satellites.

of satellites, $\dot{r}_1$ and $\dot{r}_2$ represent the absolute velocity of double satellites, respectively; $\dot{\rho}_{12}=\dot{\boldsymbol{r}}_{12}\cdot\boldsymbol{e}_{12}$ shows the range-rate of the K-band range-rate system along the track, $\dot{\boldsymbol{r}}_{12}=\dot{\boldsymbol{r}}_2-\dot{\boldsymbol{r}}_1$ expresses the relative velocity vector between twin satellites, and $\boldsymbol{e}_{12}=\boldsymbol{r}_{12}/|\boldsymbol{r}_{12}|$ indicates the unit vector identifying the direction to the second satellite from the first; $T_2-T_1=\dfrac{\partial T}{\partial\phi}\Delta\phi$ shows the disturbing geopotential difference of double satellites, $\Delta\phi=\dfrac{\rho_{12}}{r}$, where ρ_{12} denotes the inter-satellite range. The power spectrum of $\dot{\rho}_{12}$ is expressed as

$$P_l^2\{\dot{\rho}_{12}\}=\frac{r}{GM}P_l^2\left\{\frac{\partial T(r,\phi,\lambda)}{\partial\phi}\right\}(\Delta\phi)^2. \tag{11}$$

Combining Eqs.(5) and (8) with Eq.(11), the relationship between cumulative geoid height error $\delta N_{\dot{\rho}}$ and inter-satellite range-rate error $\delta\dot{\rho}_{12}$ can be expressed as

$$\delta N_{\dot{\rho}_{12}}=R_{\mathrm{e}}\sqrt{\frac{R_{\mathrm{e}}}{GM}\left(\frac{r}{\rho_{12}}\right)^2\sum_{l=2}^{L}\left[\frac{2}{l^2}\left(\frac{r}{R_{\mathrm{e}}}\right)^{2l+1}\sigma_l^2(\delta\dot{\rho}_{12})\right]}. \tag{12}$$

2.2. Orbital position error model

The relationship between the centripetal acceleration $\ddot{r}$ and linear velocity $\dot{r}$ of a satellite can be given by

$$\ddot{r}=\frac{\dot{r}^2}{r}, \tag{13}$$

where $\ddot{r}=\ddot{r}_{\rho_{12}}/\sin(\Delta\phi/2)$, $\ddot{r}_{\rho_{12}}$ denotes the along-track component of $\ddot{r}$. Equation (13) is rewritten as

$$\ddot{r}_{\rho_{12}}=\frac{\sin(\Delta\phi/2)}{r}\dot{r}^2. \tag{14}$$

Differentiating Eq.(14) on both sides yields

$$\mathrm{d}\ddot{r}_{\rho_{12}}=\frac{2\dot{r}\sin(\Delta\phi/2)}{r}\mathrm{d}\dot{r}, \tag{15}$$

where $\dot{r}=\sqrt{GM/r}$. Multiplying Eq.(15) by time t on both sides results in

$$\mathrm{d}\dot{r}_{\rho_{12}}=\sqrt{\frac{4GM\sin^2(\Delta\phi/2)}{r^3}}\mathrm{d}r. \tag{16}$$

Based on Eq.(16), the relationship between inter-satellite range-rate error $\delta\dot{\rho}_{12}$ and orbital position error δr can be shown to be

$$\delta\dot{\rho}_{12}=\sqrt{\frac{4GM\sin^2(\Delta\phi/2)}{r^3}}\delta r. \tag{17}$$

Substituting Eq.(17) into Eq.(12), the relationship between cumulative geoid height error δN_r and orbital position error δr can be expressed as

$$\delta N_r=R_{\mathrm{e}}\sqrt{\frac{R_{\mathrm{e}}}{GM}\left(\frac{r}{\rho_{12}}\right)^2\sum_{l=2}^{L}\left[\frac{2}{l^2}\left(\frac{r}{R_{\mathrm{e}}}\right)^{2l+1}\sigma_l^2\left(\sqrt{\frac{4GM\sin^2(\Delta\phi/2)}{r^3}}\delta r\right)\right]}. \tag{18}$$

2.3. Orbital velocity error model

As shown in Fig.2, the relationship between $\ddot{r}_{\rho_{12}}$ and $\ddot{r}$ can be shown to be

$$\ddot{r}_{\rho_{12}}=\ddot{r}\sin(\Delta\phi/2). \tag{19}$$

Differentiating Eq.(19) on both sides yields

$$\mathrm{d}\ddot{r}_{\rho_{12}} = \sin(\Delta\phi/2)\mathrm{d}\ddot{r}, \tag{20}$$

Multiplying Eq.(20) by time t on two sides yields

$$\mathrm{d}\dot{r}_{\rho_{12}} = \sin(\Delta\phi/2)\mathrm{d}\dot{r}. \tag{21}$$

Based on Eq.(21), the relationship between inter-satellite range-rate error $\delta\dot{\rho}_{12}$ and orbital velocity error $\delta\dot{r}$ can be given by

$$\delta\dot{\rho}_{12} = \sin(\Delta\phi/2)\delta\dot{r}. \tag{22}$$

Substituting Eq.(22) into Eq.(12), the relationship between cumulative geoid height error $\delta N_{\dot{r}}$ and orbital velocity error $\delta\dot{r}$ can be expressed as

$$\delta N_{\dot{r}} = R_{\mathrm{e}}\sqrt{\frac{R_{\mathrm{e}}}{GM}\left(\frac{r}{\rho_{12}}\right)^2\sum_{l=2}^{L}\left[\frac{2}{l^2}\left(\frac{r}{R_{\mathrm{e}}}\right)^{2l+1}\sigma_l^2(\sin(\Delta\phi/2)\delta\dot{r})\right]}. \tag{23}$$

2.4. Non-conservative force error model

Because the main direction of non-conservative force is approximately the same as the inter-satellite range-rate and non-conservative force usually represents the cumulative characteristics of error, based on the integral square error principle, the relationship between inter-satellite range-rate error $\delta\dot{\rho}_{12}$ and non-conservative force error δf is given by

$$\delta\dot{\rho}_{12} = \sqrt{\int(\delta f)^2\mathrm{d}t}. \tag{24}$$

Substituting Eq.(24) into Eq.(12), the relationship between cumulative geoid height error δN_f and non-conservative force error δf can be expressed as

$$\delta N_f = R_{\mathrm{e}}\sqrt{\frac{R_{\mathrm{e}}}{GM}\left(\frac{r}{\rho_{12}}\right)^2\sum_{l=2}^{L}\left[\frac{2}{l^2}\left(\frac{r}{R_{\mathrm{e}}}\right)^{2l+1}\sigma_l^2\left(\sqrt{\int(\delta f)^2\mathrm{d}t}\right)\right]}. \tag{25}$$

2.5. Combined error model

According to Eqs.(12), (18), (23) and (25), the combined error model of cumulative geoid height influenced by four error sources including inter-satellite range rate, orbital position, orbital velocity and non-conservative force can be established as

$$\delta N = R_{\mathrm{e}}\sqrt{\frac{R_{\mathrm{e}}}{GM}\left(\frac{r}{\rho_{12}}\right)^2\sum_{l=2}^{L}\left[\frac{2}{l^2}\left(\frac{r}{R_{\mathrm{e}}}\right)^{2l+1}\sigma_l^2(\delta\eta)\right]}, \tag{26}$$

where

$$\delta\eta = \sqrt{\sigma_l^2(\delta\dot{\rho}_{12}) + \sigma_l^2\left(\sqrt{\frac{4GM\sin^2(\Delta\phi/2)}{r^3}}\delta r\right) + \sigma_l^2(\sin(\Delta\phi/2)\delta\dot{r}) + \sigma_l^2\left(\sqrt{\int(\delta f)^2\mathrm{d}t}\right)}.$$

Based on the semi-analytical approach, the processes of estimating cumulative geoid height error using the combined error model are shown as follows (e.g. for GRACE Follow-On):

Firstly, the ephemerides of GRACE Follow-On are simulated based on the numerical integral formulas of the 9th-order Runge–Kutta linear single-step method together with the 12th-order Adams–Cowell linear multi-step method. The orbital parameters are shown in Table 1, the simulated orbit is shown in Fig.3, and the numerical simulation of orbital data takes about 3 hours.

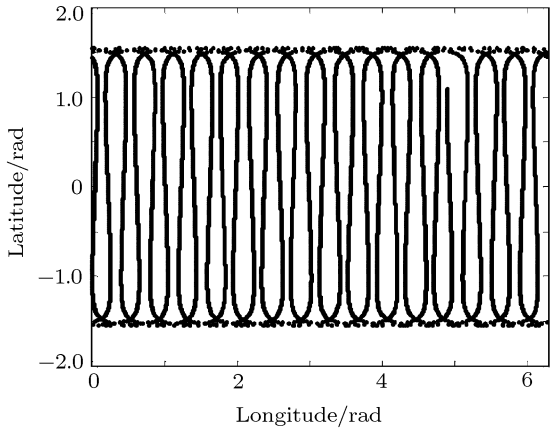


Fig.3. Simulated orbit of GRACE Follow-On satellite.

Secondly, the stochastic noises $\delta\eta$ of normal distribution with time span of 30 d and sample interval of 10 s are produced based on $\delta\dot{\rho}_{12}$, δr, $\delta\dot{r}$ and δf.

Thirdly, the grids with a $1^\circ \times 1^\circ$ resolution are plotted on an orbital reference sphere of longitude λ (0°–360°) and latitude ϕ (-90°–90°), and $\delta\eta$ is put in the track position of orbit on the reference sphere. As shown in Fig.4, $\delta\eta(\phi,\lambda)$ is reduced averagely to the grids, where horizontal and vertical coordinates represent respectively longitude and latitude, and the darkness shows $\delta\eta(\phi,\lambda)$ reduced averagely to the grids (nm/s). In this study, we estimate the accuracy of the global gravitational field using different resolutions of grid $0.1^\circ \times 0.1^\circ$–$10^\circ \times 10^\circ$ on the orbital reference sphere. The results show that with the increase of grid resolution, the reduced errors including continuation error and gridding error will be reduced, but computing time will be enhanced step by step. When the grid resolution is designed to be $1^\circ \times 1^\circ$, the reduced error is about 10^{-10} m/s, which does not influence substantively the accuracy of the global gravitational field by the premise of guaranteeing computing speed.

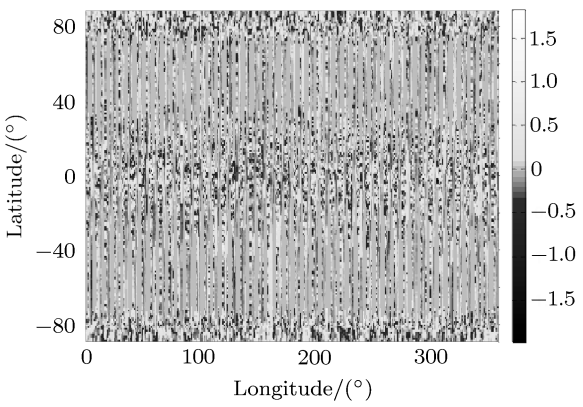


Fig.4. Distribution of $\delta\eta$ (nm/s) on orbital reference sphere from GRACE Follow-On.

Finally, according to the spherical harmonic function, $\delta\eta(\phi,\lambda)$ is expanded as

$$\delta\eta(\phi,\lambda) = \sum_{l=0}^{L}\sum_{m=0}^{l}[(C_{\delta\eta_{lm}}\cos m\lambda + S_{\delta\eta_{lm}}\sin m\lambda) \times \bar{\mathrm{P}}_{lm}(\sin\phi)], \tag{27}$$

where $C_{\delta\eta_{lm}}$ and $S_{\delta\eta_{lm}}$ denote the expanded coefficients of $\delta\eta(\phi,\lambda)$

$$(C_{\delta\eta_{lm}}, S_{\delta\eta_{lm}}) = \frac{1}{4\pi}\iint[\delta\eta(\phi,\lambda)\bar{\mathrm{Y}}_{lm}(\phi,\lambda)\cos\phi \mathrm{d}\phi\mathrm{d}\lambda]. \tag{28}$$

The variance of $\delta\eta$ at every degree is expressed as

$$\sigma_l^2(\delta\eta) = \sum_{m=0}^{l}(C_{\delta\eta_{lm}}^2 + S_{\delta\eta_{lm}}^2). \tag{29}$$

Substituting Eq.(29) into Eq.(26), the accuracy of the global gravitational field can be accurately and rapidly estimated using $\delta\eta$.

3. Results

Figure 5 illustrates a comparison of cumulative geoid height errors up to degree and order 360 using the accuracy indexes of GRACE Follow-On key payloads (shown in Table 2). The solid, dashed thin, dashed bold and circle lines represent cumulative geoid height errors based on, respectively, the inter-satellite range-rate error of the interferometric laser ranging system, the orbital position and velocity errors of GPS receiver and the non-conservative force error of the accelerometer using the semi-analytical approach. The conformance of four curves at every degree can validate that the accuracy indexes of key payloads match one another.

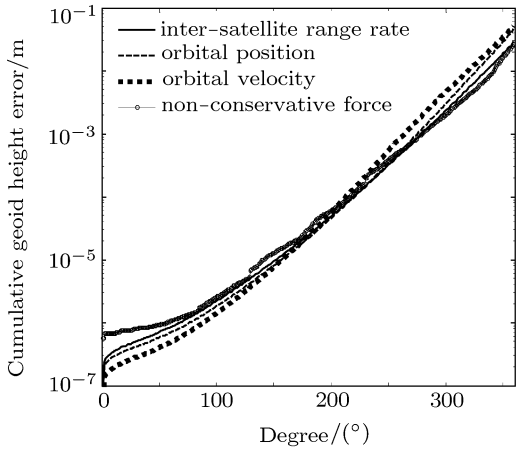


Fig.5. A comparison of cumulative geoid height errors based on the accuracy indexes of GRACE Follow-On key payloads.

Table 2. Accuracy indexes from GRACE and GRACE Follow-On key payloads.

parameters	accuracy indexes	
	GRACE	GRACE Follow-On
inter-satellite rang rate	1×10^{-6}/m·s^{-1}	1×10^{-9}/m·s^{-1}
orbital position	3×10^{-2}/m	3×10^{-5}/m
orbital velocity	5×10^{-5}/m·s^{-1}	5×10^{-8}/m·s^{-1}
non-conservative force	3×10^{-10}/m·s^{-2}	3×10^{-13}/m·s^{-2}

Figure 6 compares cumulative geoid height errors from GRACE and GRACE Follow-On for the same inter-satellite range 50 km and different orbital altitudes based on the semi-analytical approach. The statistical results of cumulative geoid height error from GRACE and GRACE Follow-On for different satellite orbital altitudes at every degree are shown in Table 3.

As shown in Fig.6, the cross line expresses the accuracy of Earth's gravitational field model EIGEN-GRACE02S complete up to degree and order 120 which is provided by the GeoForschungsZentrum Potsdam (GFZ) in Germany, and cumulative geoid height error is 1.839×10^{-1} m at degree 120. The dashed thin line represents the cumulative geoid height error using GRACE Level 1B measured observation errors of the year 2007 from key payloads published by the Jet Propulsion Laboratory (JPL), (shown in Table 2), and cumulative geoid height error is 1.985×10^{-1} m at degree 120. The conformance of two curves at every degree confirms that the combined error model is completely dependable.

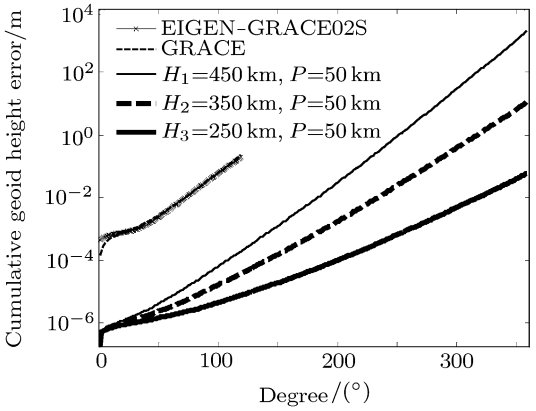


Fig.6. A comparison of cumulative geoid height errors from GRACE and GRACE Follow-On with different orbital altitudes.

Table 3. The statistics of cumulative geoid height error at every degree from GRACE and GRACE Follow-On.

degrees	Cumulative geoid height errors (m)				
	EIGEN-GRACE02S	GRACE	GRACE Follow-On		
			450/km	350/km	250/km
50	2.282×10^{-3}	2.505×10^{-3}	3.920×10^{-6}	2.253×10^{-6}	1.406×10^{-6}
80	1.566×10^{-2}	1.524×10^{-2}	1.878×10^{-5}	6.709×10^{-6}	2.606×10^{-6}
100	5.756×10^{-2}	5.682×10^{-2}	5.955×10^{-5}	1.562×10^{-5}	4.356×10^{-6}
120	1.839×10^{-1}	1.985×10^{-1}	1.916×10^{-4}	3.725×10^{-5}	7.573×10^{-6}
200	–	–	2.790×10^{-2}	1.633×10^{-3}	9.629×10^{-5}
300	–	–	2.696×10^{1}	3.571×10^{-1}	4.602×10^{-3}
360	–	–	2.077×10^{3}	1.125×10^{1}	5.825×10^{-2}

As shown in Fig.6, the solid bold, dashed bold and solid thin lines denote, respectively, the cumulative geoid height errors from GRACE Follow-On with different satellite orbital altitudes 250 km, 350 km and 450 km. At degree 360, the cumulative geoid height error is 5.825×10^{-2} m at altitude 250 km, is 193 times enhanced at altitude 350 km, and is 35656 times improved at altitude 450 km. The results are shown as follows: with the increase of satellite orbital altitude (250–450 km), the accuracy of the global gravitational field is reduced rapidly. Accordingly, one of the three key reasons why the accuracy of the global gravitational field from GRACE Follow-On ($\sim$ 250 km) is at least one order of magnitude higher than that from GRACE ($\sim$ 450 km) is that satellite orbital altitude from GRACE Follow-On is deceased sharply, and then the attenuation of global gravitational field with the increase of orbit altitude is effectively suppressed. The other two reasons are that GRACE Follow-On greatly improves the accuracy of inter-satellite range-rate by the interferometric laser ranging system and compensates very accurately the non-conservative force acting

on twin satellites by the drag-free control system.

4. Conclusions

The 21st century is a new epoch during which human beings upgrade cognitive abilities for "Digital Earth" using the Satellite-to-Satellite Tracking (SST) and Satellite Gravity Gradiometry (SGG) techniques. In this study, we set up the new combined error model of cumulative geoid height influenced by four error sources including inter-satellite range-rate, orbital position, orbital velocity and non-conservative force, based on the power spectrum principle in physics using the semi-analytical approach. We also put forward the matching relationship of accuracy indexes from GRACE Follow-On key payloads, validate the dependability of the combined error model using GRACE Level 1B observation errors measured in 2007, and demonstrate the feasibility of high-accuracy and rapid global gravitational field estimation to be made by the future GRACE Follow-On mission.

Because GRACE and GRACE Follow-On key payloads (K-band/interferometric laser ranging system, GPS receiver and accelerometer) noises are the most important error sources, the studies in this paper mainly focus on the influences of key payloads on the accuracy of global gravitational field estimation. This work can not only provide a theoretical foundation and calculational guarantee for the high-accuracy measurement of current GRACE and the optimal design of future GRACE Follow-On, but also may give some guide to the improvement of international satellite gravity measurement. Future studies may be possible by appropriately considering other correction models, including tide, ocean, atmospheric and so on, to improve the accuracy of global gravitational field measurement.

Acknowledgements

The authors would like to thank the American NASA, JPL and German GFZ for providing relevant information of the GRACE and GRACE Follow-On missions. We greatly appreciate the helpful and constructive discussion from professor Luo J, School of Physics, Huazhong University of Science and Technology, China and Dr. Xu P L, Disaster Prevention Research Institute, Kyoto University, Japan.

References

[1] Zhu Z H, Ge P W, Xu Z Y and Huo C R 1998 *Chin. Phys.* **7** 801
[2] Liu Y C, Chen W C, Huo C R and Ge P W 1999 *Chin. Phys.* **8** 881
[3] Zhu Z H, Ge P W and Xu Z Y 2000 *Chin. Phys.* **9** 321
[4] Wei Z Q 2001 *Annual Conference of China Association for Science and Technology — Geoscience and Observation Technology* 264 (in Chinese)
[5] Wu X P 2001 *Engineering of Surveying and Mapping* **10** 1 (in Chinese)
[6] Xu H Z 2001 *Science of Surveying and Mapping* **26** 1 (in Chinese)
[7] Chen G 2001 *Chin. Phys.* **10** 787
[8] Ning J S 2002 *Journal of Geodesy and Geodynamics* **22** 1 (in Chinese)
[9] Wu Y B, Li J L and Li L 2002 *Chin. Phys.* **11** 222
[10] Zhu Z H, Hong Y, Ge P W and Yu Y D 2004 *Chin. Phys.* **13** 1982
[11] Zheng W, Shao C G and Luo J 2004 *Progress of Geodesy and Geodynamics* **328** (in Chinese)
[12] Shen Y Z, Xu H Z and Wu Bin 2005 *Chin. J. Geophys.* **48** 80
[13] Zheng W, Lu X L, Xu H Z, Shao C G, Luo J and Wang N C 2005 *Prog. Nat. Sci.* **15** 596
[14] Zheng W, Shao C G, Luo J and Xu H Z 2006 *Chin. J. Geophys.* **49** 712
[15] Zheng W 2007 *Ph.D. Dissertation* (Wuhan: Huazhong University of Science and Technology) (in Chinese)
[16] Xu P L 2008 *Celest. Mech. Dyn. Astron.* **100** 231
[17] Zeng X X, Yang S Z and Chen D Y 2008 *Chin. Phys.* B **17** 1629
[18] Zheng W, Xu H Z, Zhong M and Yun M J 2008 *Chin. Phys. Lett.* **25** 4482
[19] Zheng W, Shao C G, Luo J and Xu H Z 2008 *Prog. Nat. Sci.* **18** 555
[20] Zheng W, Xu H Z, Zhong M, Yun M J, Zhou X H and Peng B B 2008 *Chin. J. Geophys.* **51** 1704
[21] Zheng W, Xu H Z, Zhong M and Yun M J 2009 *Journal of Geodesy and Geodynamics* **29** 100 (in Chinese)
[22] Zheng W, Xu H Z, Zhong M, Yun M J, Zhou X H and Peng B B 2009 *Chin. J. Geophys.* **52** in press
[23] Zheng W, Xu H Z, Zhong M and Yun M J 2009 *Chin. Phys. Lett.* **26** 029101-1
[24] Zheng W, Xu H Z, Zhong M and Yun M J 2009 *Science of Surveying and Mapping* **34** in press (in Chinese)
[25] Cazenave A and Nerem R S *Science* **297** 783
[26] Zhong M, Naito I and Kitoh A 2003 *J. Geophys. Res.* **108** 2057
[27] Han S C, Shum C K, Bevis M, Ji C and Kuo C Y 2006 *Science* **313** 658
[28] Loomis B, Nerem R S, Rowlands D and Luthcke S 2006 *American Geophysical Union, Fall Meeting* Austin: University of Texas
[29] Watkins M 2006 *American Geophysical Union, Fall Meeting*, Austin: University of Texas
[30] Jekeli C and Rapp R H 1980 *OSU Report* No. 307, Ohio State University